RIN2 Deficiency Results in Macrocephaly, Alopecia, Cutis Laxa, and Scoliosis: MACS Syndrome

Lina Basel-Vanagaite,[1,2,14] Ofer Sarig,[4,14] Dov Hershkovitz,[6,7] Dana Fuchs-Telem,[2,4] Debora Rapaport,[3] Andrea Gat,[5] Gila Isman,[4] Idit Shirazi,[4] Mordechai Shohat,[1,2] Claes D. Enk,[10] Efrat Birk,[2] Jürgen Kohlhase,[11] Uta Matysiak-Scholze,[11] Idit Maya,[1] Carlos Knopf,[9] Anette Peffekoven,[12] Hans-Christian Hennies,[12] Reuven Bergman,[8] Mia Horowitz,[3] Akemi Ishida-Yamamoto,[13] and Eli Sprecher[2,4,6,*]

Inherited disorders of elastic tissue represent a complex and heterogeneous group of diseases, characterized often by sagging skin and occasionally by life-threatening visceral complications. In the present study, we report on an autosomal-recessive disorder that we have termed MACS syndrome (macrocephaly, alopecia, cutis laxa, and scoliosis). The disorder was mapped to chromosome 20p11.21-p11.23, and a homozygous frameshift mutation in *RIN2* was found to segregate with the disease phenotype in a large consanguineous kindred. The mutation identified results in decreased expression of RIN2, a ubiquitously expressed protein that interacts with Rab5 and is involved in the regulation of endocytic trafficking. RIN2 deficiency was found to be associated with paucity of dermal microfibrils and deficiency of fibulin-5, which may underlie the abnormal skin phenotype displayed by the patients.

Disorders of elastic tissue often share common phenotypic features, including redundant skin, hyperlaxity of joints, and, in severe cases, rupture of hollow body organs, with catastrophic consequences.[1,2] The prototype for this type of abnormality is cutis laxa (CL), a heterogeneous group of acquired and inherited disorders characterized by redundant, loose, and inelastic skin.[3] CL can be present at birth or appear at different stages of growth and development. Genetic forms of CL include autosomal-recessive CL type I (ARCL1 [MIM 219100]), autosomal-recessive CL type II (ARCL2 [MIM 219200]), X-linked CL, also known as X-linked occipital horn syndrome (OHS [MIM 304150]), and autosomal-dominant CL (ADCL MIM 123700). ARCL1 is usually severe or even lethal in childhood as a result of pulmonary emphysema and cardiovascular complications and can be caused by mutations in the *FBLN4* (MIM 603634) and *FBLN5* (MIM 604580) genes, encoding fibulin-4 and -5, respectively.[4–6] *FBLN4* mutations are also associated with bone fractures, vascular tortuosity, aortic aneurysm, emphysema, hernias, joint laxity, and pectus excavatum. ADCL is caused by mutations in the *ELN* (MIM 130160) gene,[7] which encodes elastin. Fibulins are part of the microfibrillar component of the elastic fibers and form a structural backbone onto which amorphous elastin is deposited, explaining the overlapping phenotype resulting from mutations affecting both elastin and fibulin genes.[8] ARCL2 is caused by mutations in the *ATP6V0A2* (MIM 611716) gene, and these mutations have been shown to result in decreased secretion of elastin.[9,10] In addition, several other autosomal-recessive syndromes, characterized by redundant skin and additional clinical features, have been reported, including Ehlers Danlos syndrome type VII (MIM 225410), caused by mutations in the *PLOD1* (MIM 153454) gene,[11] and de Barsy syndrome (MIM 219150),[12] whose etiology is still unknown. Growth retardation, alopecia, pseudoanodontia, and optic atrophy (GAPO [MIM 230740]) syndrome is characterized by redundant appearance of facial skin (but not of other areas of the body), short stature, alopecia, pseudoanodontia, various eye abnormalities (including optic atrophy and glaucoma), and a typical facial dysmorphism.[13–17] Here, too, the etiology of the syndrome remains elusive.

In the present report, we studied a new syndrome related to the CL group of inherited disorders. The patients with this syndrome are all members of two related consanguineous Israeli-Arab families and were all born with normal birth weights after full-term, uneventful pregnancies. Psychomotor development was normal. On clinical examination, macrocephaly (Figures 1A and 1B), downward-slanting palpebral fissures, puffy eyelids (Figures 1A and 1B), mild ichthyosis (Figure 1C), sagging cheeks, everted lower lip, retrognathia with abnormal skull morphology (Figure 1D), gingival hyperplasia (Figure 1G), abnormal position of the teeth (Figures 1G and 1H), severe hyperlaxity, and flat feet were observed. Unfortunately, no data on the occipitofrontal circumference (OFC) at birth or on the

[1]Schneider Children's Medical Center of Israel and Raphael Recanati Genetics Institute, Rabin Medical Center, Beilinson Campus, 49100 Petah Tiqva, Israel; [2]Sackler Faculty of Medicine, [3]Department of Cell Research and Immunology, Tel Aviv University, 69978 Ramat Aviv, Israel; [4]Department of Dermatology, [5]Department of Pathology, Tel Aviv Sourasky Medical Center, 64289 Tel Aviv, Israel; [6]Center for Translational Genetics, Rappaport Institute and Faculty of Medicine, Technion – Israel Institute of Technology, 31096 Haifa, Israel; [7]Department of Pathology, [8]Department of Dermatology, [9]Metabolic Disease Unit, Meyer Children's Hospital, Rambam Health Care Campus, 31096 Haifa, Israel; [10]Department of Dermatology, Hadassah Hebrew University Medical School, 91120 Jerusalem, Israel; [11]Center for Human Genetics, 79100 Freiburg, Germany; [12]Division of Dermatogenetics, Cologne Center for Genomics, University of Cologne, 50674 Cologne, Germany; [13]Department of Dermatology, Asahikawa Medical College, 078-8510 Asahikawa, Japan
[14]These authors contributed equally to this work
*Correspondence: elisp@tasmc.health.gov.il
DOI 10.1016/j.ajhg.2009.07.001.

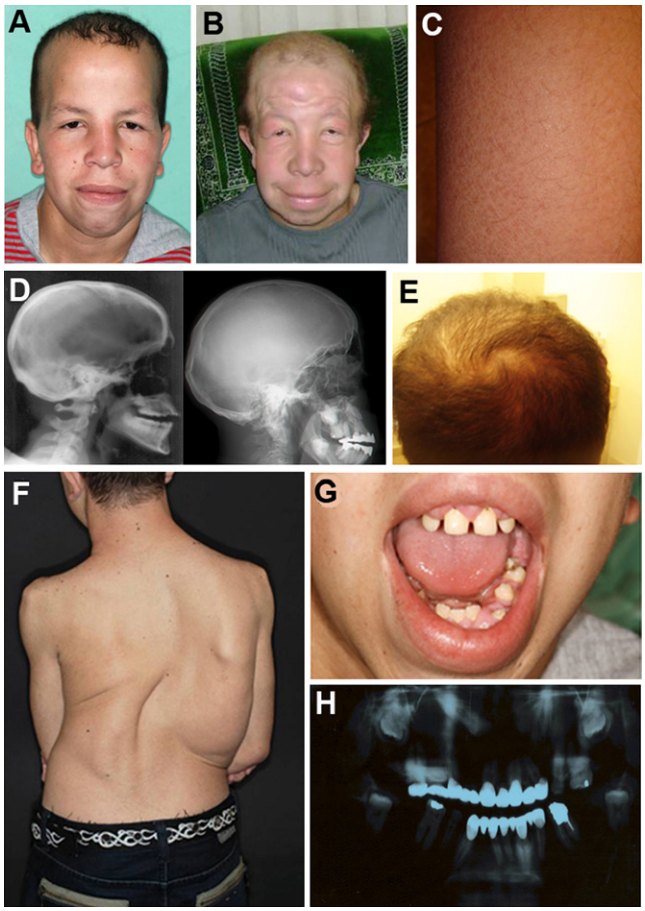

Figure 1. Clinical Phenotype
(A and B) Facial appearance of patients II-4 (A) and II-5 (B). Note age-dependant worsening of the sagging skin phenotype.
(C) Mild ichthyosis can be seen in patient II-4.
(D) Skull radiographs of a normal individual (left) and of a patient (right).
(E) Short and sparse hair can be seen in patient II-5.
(F) Severe kyphoscoliosis can be seen in patient II-4.
(G) Irregularly placed teeth and gingival hypertrophy can be seen in patient II-4.
(H) Panoramic X-ray of the oral cavity in patient II-5, demonstrating unerupted wisdom and upper canine teeth.

timing of closure of the fontanelles were available. There has been no progression of the macrocephaly over the past two years in patient II-4.

The phenotype also included coarse and swollen facial appearance affecting the eyelids, lips, and cheeks. Skin laxity was more apparent in the facial than in the abdominal area (Figures 1A and 1B). Scalp hair was sparse (Figure 1E). Short stature was caused mainly by moderate to severe scoliosis in all three affected individuals (Figure 1F).

The facial phenotype in the two older affected family members (II-5 and II-6) was more prominent, including sagging eyelids and sagging cheeks, as compared with that of the youngest patient (II-4) (Figures 1A and 1B).

Easy bruising, atrophic scars, transparent veins, and blue sclera were not observed. The patients denied respiratory problems or any other systemic complaints, except for severe back pain in the youngest affected family member, who displayed severe kyphoscoliosis on examination (Figure 1F). Neurological examination was normal. Eye examination, including fundus, was normal in patients II-4 and II-8. The clinical features of all affected family members are summarized in Table 1.

Complete blood counts, renal and liver function tests, and thyroid stimulating hormone (TSH) level were all normal. A skeletal X-ray survey of patient II-4 revealed severe scoliosis. On echocardiography, mild dilatation of the aorta was detected in patient II-4. Panoramic X-ray of the teeth in patient II-5 demonstrated unerupted wisdom and canine teeth (Figure 1H). A bone density scan in patient II-5 revealed generalized osteoporosis, more severe in the spine. Serum transferrin isoform analysis was not suggestive of a congenital glycosylation defect. In addition, isoelectric focusing analysis revealed a normal apolipoprotein CIII profile (Apo $CIII_2 = 48\%$, Apo $CIII_1 = 49\%$, Apo $CIII_0 = 3\%$).

Light microscopic examination of skin biopsies obtained from patients II-4 and II-5 revealed a normal epidermis. In the papillary (upper) dermis, elastic fibers were sparse, with an almost complete absence of oxytalin fibers (Figures 2A–2D). With the use of Verhoeff's Van Gieson staining, elastic fibers appeared normally distributed in the reticular (lower) dermis (Figure 2E). Collagen fiber structure and distribution appeared normal throughout the skin (Figure 2F). Minimal focal interstitial mucin deposition was detected with Alcian blue staining (not shown).

Transmission electron microscopy of dermal elastic fibers demonstrated diminished microfibrillar component at the periphery of elastic fibers (Figure 2G). These findings correlated with markedly decreased staining for fibulin-5, a major component of dermal elastic microfibrils (Figures 2H and 2I). We did not observe any abnormalities in lysosome appearance with the use of electron microscopy. In addition, the patients did not show clinical signs of lysosomal storage disease (neurological abnormalities, hepatosplenomegaly, thrombocytopenia, progressive disease course, dysostosis multiplex on skeletal X-rays, etc…).

Scanning electron microscopy examination of hair obtained from affected patients showed no abnormalities (not shown).

Taken altogether, the unique constellation of signs displayed by the patients reported in this study demarcates a clinically new syndrome, which we have termed MACS syndrome—for macrocephaly, alopecia, cutis laxa, and scoliosis.

Genomic DNA was extracted from leukocytes from peripheral venous blood in EDTA, with the use of standard procedures, after informed consent was obtained from all family members or their legal guardians, in accordance with a protocol approved and reviewed by the National Committee for Genetic Studies, Israel Ministry of Health. We genotyped affected family members, using Affymetrix Human Mapping NspI 250K arrays in accordance with the manufacturer's instructions, and identified a continuous segment of homozygosity shared by the patients and encompassing 815 consecutive SNPs over 6.8 Mb between

Table 1. Clinical Features of the Patients

	Patient II-4	Patient II-5	Patient II-6
General and familial data			
Birth weight (g)	3500	NA	NA
Age (yrs)	15	32	35
Height (cm) (SD)	149 (−2)	165 (−1.5)	NA
Maternal height (cm) (SD)	160 (0)		
Paternal height (cm) (SD)	167 (−1)		
Weight (kg) (SD)	44 (−2)	47 (−2.5)	NA
OFC (cm) (SD)	59.5 (+3)	58.5 (+2)	NA
Maternal OFC (cm) (SD)	56.5 (+1.5)		
Paternal OFC (cm) (SD)	57 (+1.5)		
Facial characteristics			
Downslanting palpebral fissures	+	+	+
Puffy droopy eyelids	+	+	+
Full, everted lips	+	+	+
Skin characteristics			
Soft, redundant skin (especially facial)	+	+	+
Gum hypertrophy	+	+	+
Irregular dentition	+	+	+
Hair characteristics			
Receding anterior hairline, sparse hair	+	+	+
Skeletal manifestations			
Joint hypermobility	+	+	+
Scoliosis	severe	mild	mild
Fractures	−	+	−
Other features			
Umbilical hernia	+	−	−
Eye abnormalities	−	−	NA
Genitourinary abnormalities	Urethral stenosis, undescended testis	−	−
Abnormal (high-pitched) voice	+	+	+
Various	Ichthyosis on lower limbs, high-arched palate, mild aortic dilatation	Recurrent aphthous stomatitis, severe osteoporosis	Bone density scan NA

Abbreviations are as follows: NA, not available; OFC, occipitofrontal circumference. Plus signs and minus signs indicate presence and absence, respectively.

markers rs6034837 and rs2092468 on 20p11.21-p11.23 (Figure 3A). We then genotyped all family members for eight microsatellite markers (D20S186, D20S112, D20S475, D20S1145, D20S868, D20S101, D20S848, D20S195) spanning the disease interval. Only three of these markers were found to be informative or semi-informative. Microsatellite marker typing data were consistent with a gene locus for MACS syndrome in the 20p11.21-p11.23 chromosomal region, although the LOD score did not reach a critical value of 3 as a result of the lack of informativity of the markers typed in the region (not shown).

The candidate region was found to include 55 known or predicted genes. Given the fact that the MACS syndrome is transmitted in an autosomal-recessive fashion, and given the fact that most recessive disorders are caused by loss-of-function mutations often resulting in decreased mRNA levels, we hypothesized that screening the expression of the various genes located within the disease interval may point to candidate genes of interest. We therefore established fibroblast cell lines from punch skin biopsies obtained from two patients and four ethnically matched healthy controls. We then compared global gene

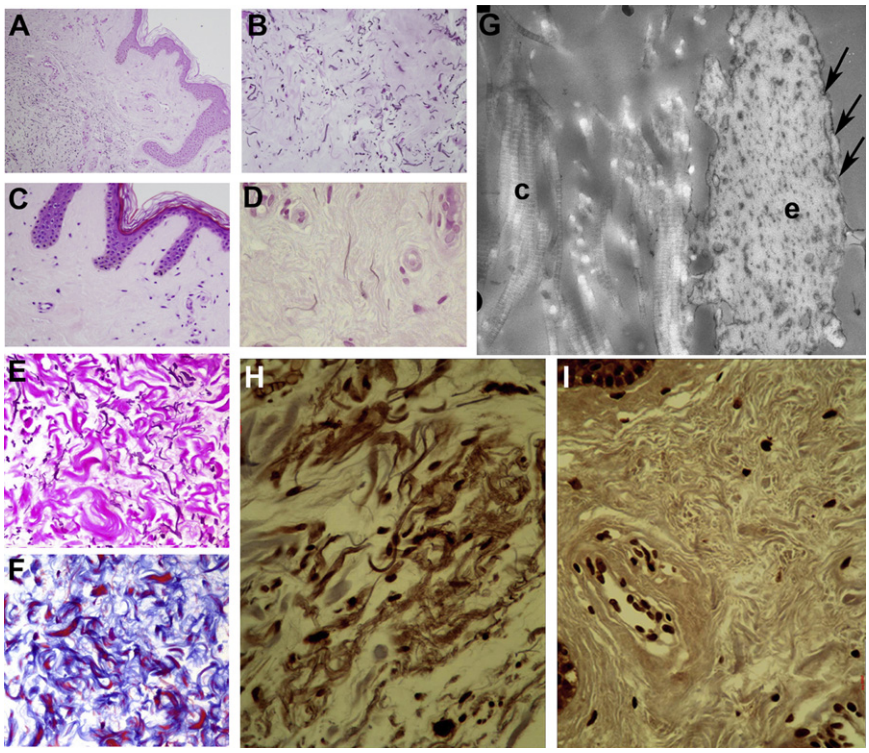

Figure 2. Pathological Features
(A–C) Histopathological examination of a skin biopsy obtained from patient II-5 (A) revealed a normal epidermis, with a striking absence of elastic fibers in the papillary dermis (C) as opposed to the reticular dermis (B).
(D) A higher magnification demonstrates almost complete absence of oxytalin fibers.
(E and F) Von Giesen (E) and Masson Trichrome (F) staining demonstrates a normal structure of elastic and collagen fibers in the reticular dermis.
(G) Transmission electron microscopy of dermal elastic fibers demonstrates diminished microfibrillar component at the periphery of elastic fibers (arrows) (e, elastic fiber; c, collagen fibers).
(H and I) Immunohistochemical staining demonstrates decreased expression of fibulin-5 in the patient dermis (I) as compared with normal skin (H).

expression, using microarrays in the six cell lines (all genes contained within the disease interval were represented on the array). Total RNA (200 ng) was reverse transcribed and cRNA prepared with the use of the TotalPrep RNA Amplification Kit (Applied Biosystems/Ambion, Austin, TX, USA), in accordance with the manufacturer's protocol. A total of 1.5 μg of biotinylated cRNA was hybridized to the Sentrix Human WG-6 v2 array (encompassing 48,701 transcript targets), washed, and scanned on a BeadArray Reader (Illumina, San Diego, CA, USA). The scanning data were exported to MatLab sofware and quantile normalized, and transcripts with a detection p value greater than 0.01 were removed from the analysis (more than 13,000 transcripts had a p value < 0.01). In the global GO term analysis, we tested all "Process" GO terms that were present in our gene set more than once. The gene set was composed from the genes that show up- or downregulation (91 up and 144 down) in fibroblast cultures established from affected subjects as compared with control fibroblasts. For each term, we randomly selected the same number of genes as appeared in our gene set and calculated each gene's frequency in this set. We repeated the process 1000 times and built a histogram of each GO term frequency. We analyzed the results with the one-sample Wilcoxon signed-ranks test to assess relative enrichment in our experimental gene set, using a cutoff of $p < 0.05$.

Out of all genes mapping to the disease interval, one, termed *RIN2* (MIM 610222), demonstrated decreased expression in both patients as compared with the nonaffected individuals (Figure 3B). *RIN2* encodes the Ras and Rab interactor 2 protein.[18,19] Supporting the relevance of the expression data to the disease phenotype, the global pathway GO term analysis of the data set (p value < 0.05) showed that many of the process terms found to be significantly enriched in the analysis were relevant to the vesicle trafficking associated with the secretory and endocytic pathways, as well as to bone development (Figure S1, available online).

RIN2 is located in the middle of the disease interval on chromosome 20p11.23, at 19,818,210-19,931,100 (UCSC Genome Browser). *RIN2* was sequenced with the use of oligonucleotide primer pairs listed in Table S1, Taq polymerase, and Q solution (QIAGEN, Valencia, CA, USA), with the following cycling conditions used: 94°C for 5 min, followed by 35 cycles at 95°C for 30 s, 57°C for 45 s, then 72°C for 1 min 30 s. Gel-purified (QIAquick Gel Extraction Kit, QIAGEN) amplicons were subjected to bidirectional DNA sequencing via the BigDye Terminator System on an ABI Prism 3100 Sequencer (PE Applied Biosystems, Foster City, CA, USA). Direct sequencing of PCR products encompassing the entire coding sequence of the gene revealed a homozygous C deletion at cDNA position 1731 (c.1731delC [p.Ile578SerfsX4]) (Figure 3C). To screen for the p.c1731delC mutation, we used forward primer 5′-CACCTACTTCGGGTGCTTAGTG-3′ and a mutation-specific reverse primer, 5′-ATTTGGTCTTCAGGGATCAGCGACTC GACG-3′, which generates a recognition site for DNA endonuclease *DrdI* in the absence of the mutation. A 183 bp fragment was PCR amplified and subsequently digested with *DrdI*. With this assay used, the mutation was found to segregate with the disease phenotype throughout the family (Figure 3D) and could be excluded from a panel of 182 ethnically matched control individuals (364 chromosomes).

We assessed the consequences of the c.1731delC mutation. For quantitative real-time RT-PCR, cDNA was

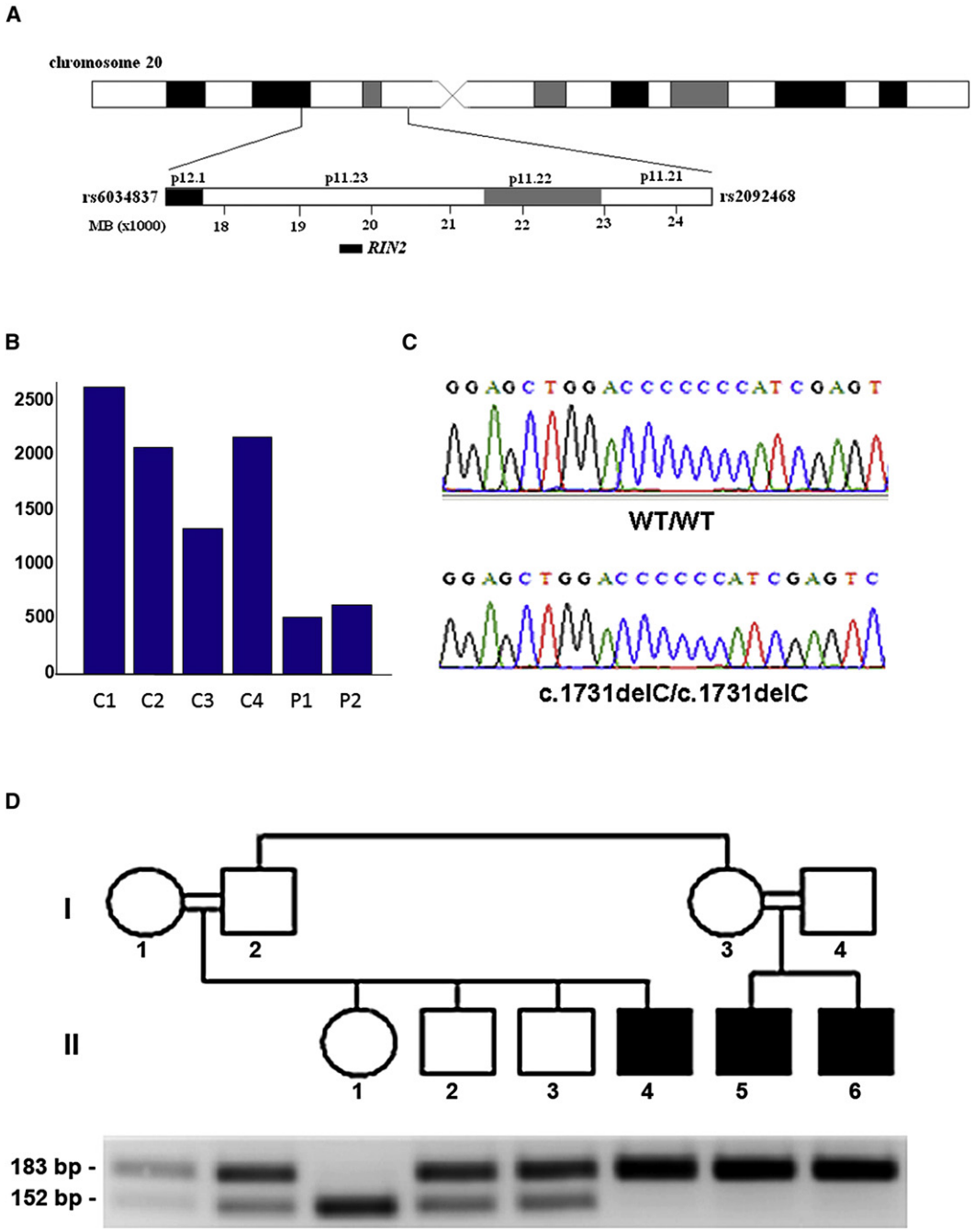

Figure 3. Mutation Identification
(A) Relative position of the disease interval and of the *RIN2* gene on 20p11.21-p11.23.
(B) Relative expression of *RIN2* in patient (P1-2) and control (C1-4) fibroblasts.
(C) Sequence analysis reveals a homozygous C deletion at cDNA position 1731 of the *RIN2* gene (lower panel). The wild-type sequence is given for comparison (upper panel).
(D) PCR-RFLP analysis confirms segregation of the mutation in the family. PCR amplification was performed as described in the text. Affected patients display a homozygous 183 bp fragment, healthy individuals show a 152 bp fragment only, but the two fragments are found in heterozygous carriers of the mutation.

synthesized from 1 μg of total RNA with the Reverse-iT First-Strand Synthesis Kit (ABgene), oligo dT, and random hexamers in a 3:1 ratio. cDNA PCR amplification was carried out with the use of SYBR Green JumpStart Taq ReadyMix (Sigma) with ROX reference dye (Sigma) on a StepOnePlus cycler (Applied Biosystems, Foster City, CA, USA), with gene-specific intron-crossing oligonucleotide pairs: 5′-CACAAACGGAGAACCACCAA-3′ and 5′-CTGA AATGCAACTCGGAGGTAAT-3′. So that the specificity of the reaction conditions was ensured, at the end of the individual runs, the melting temperature (T_m) of the amplified products was measured for confirmation of its

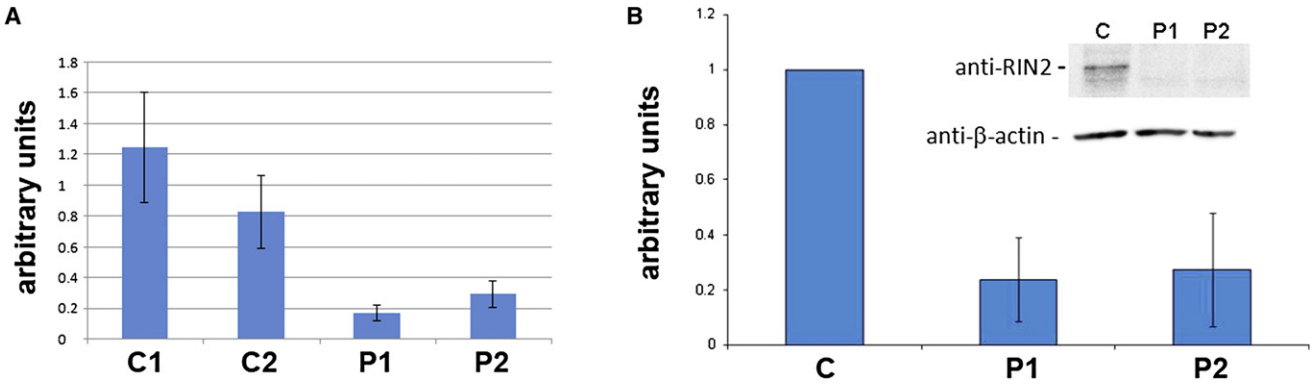

Figure 4. Consequences of the c.1731delC Mutation in RIN2

(A) Quantitative reverse transcriptase-PCR was performed on mRNA samples extracted from skin biopsies of patients (P1, P2) and healthy individuals (C1, C2).

(B) Protein was extracted from fibroblast cell cultures established from two MACS syndrome patients (P1, P2) and a control healthy individual (C) and was immunoblotted against anti-RIN2. Membranes were reblotted with anti-β-actin antibodies to control for protein loading (insert). Densitometry results are provided as arbitrary units ± SD.

homogeneity. Cycling conditions were as follows: 95°C for 3 min; 95°C for 15 s, and 60°C for 60 s, for a total of 40 cycles. Each sample was analyzed in triplicate. For quantification, standard curves were obtained with the use of serially diluted cDNA amplified in the same real-time PCR run. Results were normalized to *ACTB* and *GAPDH* mRNA levels. We found that the identified mutation resulted in markedly decreased *RIN2* mRNA levels in RNA derived from patient skin biopsies as compared with those from normal skin biopsies (Figure 4A), suggesting that the mutation induces nonsense-mRNA decay. In addition, immunoblotting of protein extracts from patient-derived fibroblasts with primary anti-RIN2 or mouse anti-β-actin (Abcam, Cambridge, MA, USA) revealed absence of the 116 kD RIN2 protein as compared with wild-type fibroblasts (Figure 4B). These data suggest that c.1731delC results in loss of function of RIN2.

Our data, therefore, clearly associate decreased expression of RIN2 to the MACS syndrome phenotype. RIN2 functions as a homophilic tetramer that is probably formed by antiparallel association of two parallel dimers.[19] The protein has 895 amino acids; it contains an SH2 domain, two proline-rich domains, a RIN homology (RH) domain, a vacuolar sorting protein 9 (Vps9) domain, and a Ras association (RA) domain.

RIN2 has been shown in vitro to function as a guanine nucleotide exchange factor (GEF) for the Rab5 protein and a stabilizer for GTP-Rab5.[19] RIN2 may in fact connect Ras to Rab5.[18] Rab proteins make up the largest class within the Ras GTPase superfamily of small GTPases and act as specific regulators of intracellular protein and membrane trafficking events.[20–22] Rab5 is involved in the initial trafficking steps of the endocytic pathway. It is required for targeting and fusion of endocytic vesicles to early endosomes.[23–26] Furthermore, Rab5 can stimulate motility of early endosomes along microtubules[27,28] and has even been shown to direct signaling from the endocytic pathway to the nucleus.[29] There are three isoforms of Rab5 (a, b, and c),[30] each with specific functions. RIN2 binds GTP preferentially over GDP and accelerates GDP-GTP exchange on RAB5b.[19] RIN2 amino acids 497–784, which contain the RH and Vps9 domains, are required for RAB5b binding. Vps9 domain-containing proteins have been shown to be implicated in human diseases. Specifically, mutations in the *ALS2* gene (amyotrophic lateral sclerosis 2 [MIM 606352]) encoding Alsin have been linked to juvenile-onset forms of the neurodegenerative diseases amyotrophic lateral sclerosis, primary lateral sclerosis, and hereditary spastic paraplegia.[31–34] The Vps9 domain of Alsin activates Rab5 and stimulates endosome fusion in vivo.[35–37]

How RIN2 deficiency results in defective elastic tissue and the skeletal abnormalities observed in MACS syndrome patients remains to be elucidated. Of interest, ARCLII and gerodermia osteodysplastica (MIM 231070), featuring both skeletal abnormalities and skin laxity, have recently been linked to abnormal Golgi trafficking.[9,10,38] It is therefore of interest that we observed accumulation of vacuoles in the Golgi system in patient fibroblasts (Figures 5A and 5B). To confirm that abnormal Golgi structure is directly due to RIN2 deficiency, we down-regulated the expression of RIN2 in normal fibroblasts by using siRNA. Here, too, we observed the appearance of numerous Golgi-associated vacuoles in RIN2-deficient fibroblasts (Figures 5C and 5D). Although RIN2 has been linked to early endosome formation, a number of intracellular pathways of importance to Golgi function, such as retrograde transport,[39] are dependant upon proper endosomal trafficking. It has been documented that RIN2 is involved in hepatocyte growth factor (HGF)-induced endocytosis of E-cadherins.[18] We, therefore, tested whether absence of RIN2 affects endocytosis of transferrin. Internalization of transferrin and its recycling from the endocytic recycling compartment (ERC) to the plasma membrane did not differ between RIN2-deficient cells and normal cells (Figure 6). Finally, no visible change in the architecture

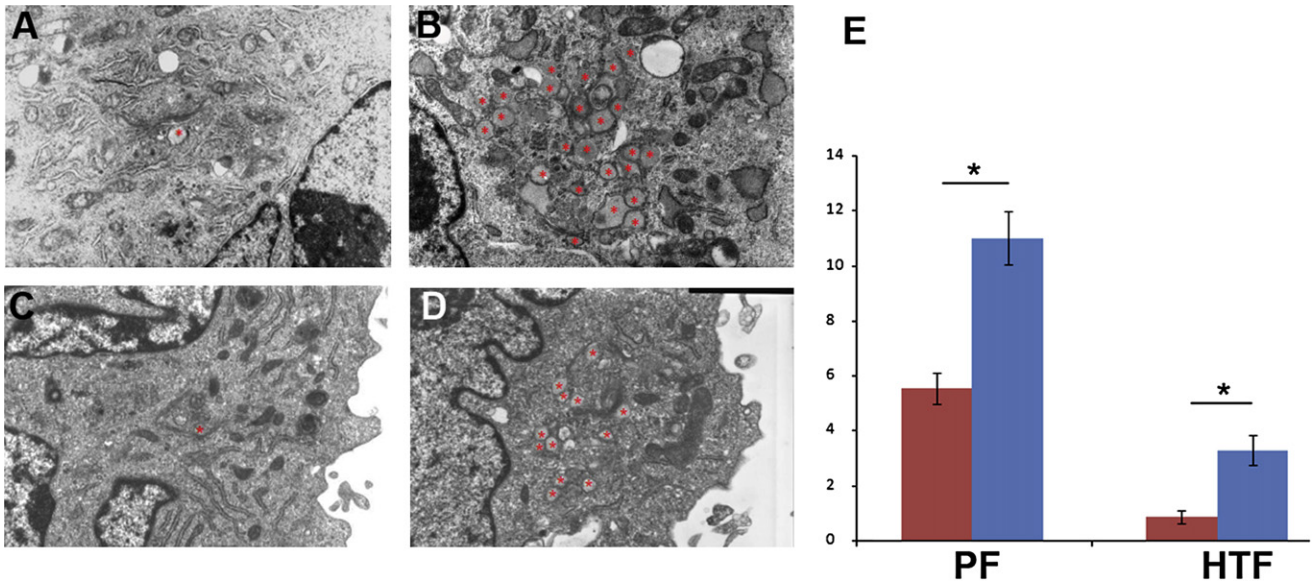

Figure 5. Ultrastuctural Consequences of RIN2 Deficiency
(A and B) Electron microscopy demonstrates numerous vacuoles (red asterisks) closely associated with the stacks of the Golgi apparatus in patient fibroblasts (B) as compared with normal fibroblasts (A).
(C and D) Numerous similar vacuoles were see in human telomerase reverse transcriptase (hTERT)-transformed fibroblasts transfected with a RIN2-specific siRNA (Sigma Oligo no. 3960234, 3960235, 3960236, 3960237) (D) as compared with the same cells transfected with a control irrelevant siRNA (C).
(E) We quantitatively compared the number of vacuoles per cell ($n = 30$) in patient (blue) versus control (red) fibroblasts (PF) and in hTERT-transformed fibroblasts (HTF) transfected with a RIN2-specific siRNA (blue) or a control siRNA (red). p values were calculated by a standard t test (asterisk indicates $p < 0.0001$).

of coated pits and coated vesicles or early endosomes was seen in RIN2-deficient cells (Figure S2).In the present study, we describe a novel autosomal recessive syndrome that we have termed MACS syndrome, for macrocephaly, alopecia, cutis laxa, and scoliosis. Because the cutaneous features of MACS syndrome were more apparent in the two older patients, it seems that the phenotype is progressive over time. This syndrome is clinically distinct from other disorders characterized by hyperlaxity and abnormal skin, including cutis laxa syndromes, various Ehlers Danlos syndrome subtypes, and the GAPO syndrome. Indeed, in contrast with ARCLI caused by *FBLN4* and *FBLN5* mutations, no visceral involvement was noted. In ARCLII, mental retardation, microcephaly, and, sometimes, pachygyria accompany skin abnormalities, and the phenotype improves over time. In addition, the fact that the abnormal appearance of the elastic tissue was restricted to the papillary dermis is very unusual for all CL types. In patients with EDS type VIIC, or dermatosparaxis, the presence of blepharochalasis and general excess of skin causes facial features highly resembling those of the patients described in this study.[40] In addition, gingival hyperplasia can be observed in EDS type VIIc, similar to that of our patients.[41] However, transparent skin and easy bruising, typical for the patients with this syndrome, were not present in our patients. Although our patients suffered from scoliosis, which is a hallmark of EDS type VI, scoliosis developed in the second decade of life in our patients, not shortly after birth as in EDS types VIa and VIb. Interestingly, some of the patients reported as having EDS syndrome type VI show facial features highly reminiscent of the features in our patients, including sagging cheeks and full puckered lips,[42] but they also show lean body habitus with arachnodactyly and no hair abnormalities. Our patients also differ from the patients with classical EDS type VI by the absence of severe hypotonia after birth and the presence of macrocephaly. Of note, our genotyping data ruled out linkage of the MACS syndrome to any of the known loci associated with EDS or CL.

GAPO syndrome is an extremely rare autosomal-recessive disease characterized by short stature, alopecia, pseudoanodontia, progressive optic atrophy, and a typical face including frontal bossing, micrognathia, protruding ears, a depressed nasal bridge and thick, full lips. More than 30 patients have been reported in the medical literature.[15] Despite striking facial similarities with GAPO syndrome patients, our patients had no eye abnormalities, and the phenotype was less severe than in most GAPO cases previously reported. We failed to identify any pathological variant within the coding sequence of *RIN2* in one family with classical GAPO syndrome and in patients of 7 families affected with cutis laxa-like phenotypes without mental retardation and without mutations in cutis laxa-associated genes (not shown), supporting the idea that MACS syndrome represents a separate clinical entity.

Cutis laxa-related phenotypes have been associated with defective biogenesis of elastic fibers: whereas ARCLI results from abnormal synthesis of the microfibrillar

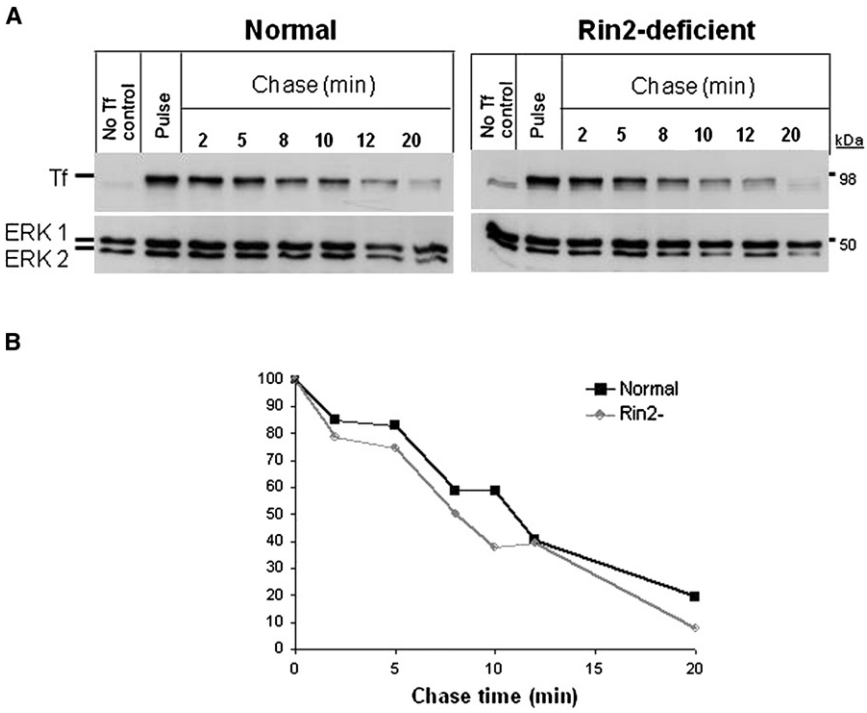

Figure 6. The Kinetics of Transferrin Recycling Are Normal in Rin2-Deficient Fibroblasts

(A) RIN2-deficient primary fibroblasts, derived from two patients (FACH and FMCH), were transformed with SV40 T-large antigen (FACHT and FMCHT). FACHT and FMCHT cells, as well as normal cells (F572T), were starved for 30 min, incubated with biotin-conjugated transferrin for 15 min, and chased for the indicated times. Equal amounts of protein lysates were subjected to SDS-PAGE, blotted, and interacted with streptavidin/HRP. Blots were reprobed with anti-ERK as a loading control. Data are representative of two independent experiments.

(B) Densitometry was used to quantitate the kinetics of biotinylated transferrin internalization and recycling. To normalize the results, we divided intensity of the transferrin band at each lane by the intensity of the total ERK (ERK1 and ERK2). The value obtained for the pulse time was considered as 100%. The results represent the mean of two independent experiments.

Abbreviations are as follows: Tf, transferrin; Rin2-, RIN2-deficient cells.

components, fibulin-4 and -5,[4–6] ARCLII has been found to result from decreased secretion of tropoelastin.[9,10] Here, we report on another cutis laxa-related disease characterized by decreased expression of fibulin-5 in the dermis. Recent data indicate that decreased fibulin expression impairs elastic fiber formation as a result of defective incorporation of elastin into the microfibril bundles and possibly as a result of diminished activation of lysyl oxidase like-1.[43]

Gerodermia osteodysplastica is an autosomal-recessive disorder characterized by wrinkly skin and osteoporosis.[44] Interestingly, patient II-5 was also found to display severe osteoporosis (Table 1). Gerodermia osteodysplastica is caused by loss-of-function mutations in *SCYL1BP1* (MIM 607983), which localizes to the Golgi apparatus and interacts with Rab6.[38] Identification of a RAB5-interacting protein as causative of the abnormal phenotype in MACS syndrome patients further demonstrates the importance of the Rab protein-related endocytic pathway in the maintenance of normal skin elasticity. The fact that decreased expression of RIN2 was found to lead to Golgi-associated abnormalities suggests the possibility that RIN2 may act along the same pathway as the golgin SCYL1BP1.

In conclusion, we have shown that a mutation in *RIN2* causes a previously unpublished inherited disorder, which we have termed MACS syndrome, demonstrating—for the first time, to our knowledge—RIN protein family involvement in a human disease. The present observations also exemplify the usefulness of combining SNP microarray-based homozygosity mapping and comparative microarray-based mRNA expression analysis to direct candidate gene screening in autosomal-recessive disorders.

Supplemental Data

Supplemental Data include two figures and one table and can be found with this article online at http://www.ajhg.org/.

Acknowledgments

We are grateful to the families who participated in this study. We also thank G. Halpern for her help with editing the manuscript.

Received: April 24, 2009
Revised: June 26, 2009
Accepted: July 1, 2009
Published online: July 23, 2009

Web Resources

The URLs for data presented herein are as follows:

Blink, http://www.ncbi.nlm.nih.gov/sutils/blink.cgi?pid=13124575
dbSNP, http://www.ncbi.nlm.nih.gov/SNP/
Ensembl Genome Browser, http://www.ensembl.org/
GenBank, http://www.ncbi.nlm.nih.gov/Genbank/
Online Mendelian Inheritance in Man (OMIM), http://www.ncbi.nlm.nih.gov/Omim/
Primer3, http://frodo.wi.mit.edu/cgi-bin/primer3/primer3_www.cgi
UCSC Genome Browser, http://genome.ucsc.edu/

References

1. Kielty, C.M. (2006). Elastic fibres in health and disease. Expert Rev. Mol. Med. *8*, 1–23.
2. Bateman, J.F., Boot-Handford, R.P., and Lamande, S.R. (2009). Genetic diseases of connective tissues: cellular and extracellular effects of ECM mutations. Nat. Rev. Genet. *10*, 173–183.

3. Ringpfeil, F. (2005). Selected disorders of connective tissue: pseudoxanthoma elasticum, cutis laxa, and lipoid proteinosis. Clin. Dermatol. *23*, 41–46.
4. Hucthagowder, V., Sausgruber, N., Kim, K.H., Angle, B., Marmorstein, L.Y., and Urban, Z. (2006). Fibulin-4: a novel gene for an autosomal recessive cutis laxa syndrome. Am. J. Hum. Genet. *78*, 1075–1080.
5. Markova, D., Zou, Y., Ringpfeil, F., Sasaki, T., Kostka, G., Timpl, R., Uitto, J., and Chu, M.L. (2003). Genetic heterogeneity of cutis laxa: a heterozygous tandem duplication within the fibulin-5 (FBLN5) gene. Am. J. Hum. Genet. *72*, 998–1004.
6. Loeys, B., Van Maldergem, L., Mortier, G., Coucke, P., Gerniers, S., Naeyaert, J.M., and De Paepe, A. (2002). Homozygosity for a missense mutation in fibulin-5 (FBLN5) results in a severe form of cutis laxa. Hum. Mol. Genet. *11*, 2113–2118.
7. Zhang, M.C., He, L., Giro, M., Yong, S.L., Tiller, G.E., and Davidson, J.M. (1999). Cutis laxa arising from frameshift mutations in exon 30 of the elastin gene (ELN). J. Biol. Chem. *274*, 981–986.
8. Hu, Q., Loeys, B.L., Coucke, P.J., De Paepe, A., Mecham, R.P., Choi, J., Davis, E.C., and Urban, Z. (2006). Fibulin-5 mutations: mechanisms of impaired elastic fiber formation in recessive cutis laxa. Hum. Mol. Genet. *15*, 3379–3386.
9. Kornak, U., Reynders, E., Dimopoulou, A., van Reeuwijk, J., Fischer, B., Rajab, A., Budde, B., Nurnberg, P., Foulquier, F., Lefeber, D., et al. (2008). Impaired glycosylation and cutis laxa caused by mutations in the vesicular H+-ATPase subunit ATP6V0A2. Nat. Genet. *40*, 32–34.
10. Hucthagowder, V., Morava, E., Kornak, U., Lefeber, D.J., Fischer, B., Dimopoulou, A., Aldinger, A., Choi, J., Davis, E.C., Abuelo, D.N., et al. (2009). Loss-of-function mutations in ATP6V0A2 impair vesicular trafficking, tropoelastin secretion, and cell survival. Hum. Mol. Genet. *18*, 2149–2165.
11. Hyland, J., Ala-Kokko, L., Royce, P., Steinmann, B., Kivirikko, K.I., and Myllyla, R. (1992). A homozygous stop codon in the lysyl hydroxylase gene in two siblings with Ehlers-Danlos syndrome type VI. Nat. Genet. *2*, 228–231.
12. Kivuva, E.C., Parker, M.J., Cohen, M.C., Wagner, B.E., and Sobey, G. (2008). De Barsy syndrome: a review of the phenotype. Clin. Dysmorphol. *17*, 99–107.
13. Demirgunes, E.F., Ersoy-Evans, S., and Karaduman, A. (2009). GAPO syndrome with the novel features of pulmonary hypertension, ankyloglossia, and prognathism. Am. J. Med. Genet. A. *149A*, 802–805.
14. Kocabay, G., and Mert, M. (2009). GAPO syndrome associated with dilated cardiomyopathy: an unreported association. Am. J. Med. Genet. A. *149A*, 415–416.
15. Goloni-Bertollo, E.M., Ruiz, M.T., Goloni, C.B., Muniz, M.P., Valerio, N.I., and Pavarino-Bertelli, E.C. (2008). GAPO syndrome: three new Brazilian cases, additional osseous manifestations, and review of the literature. Am. J. Med. Genet. A. *146A*, 1523–1529.
16. Manouvrier-Hanu, S., Largilliere, C., Benalioua, M., Farriaux, J.P., and Fontaine, G. (1987). The GAPO syndrome. Am. J. Med. Genet. *26*, 683–688.
17. Tipton, R.E., and Gorlin, R.J. (1984). Growth retardation, alopecia, pseudo-anodontia, and optic atrophy–the GAPO syndrome: report of a patient and review of the literature. Am. J. Med. Genet. *19*, 209–216.
18. Kimura, T., Sakisaka, T., Baba, T., Yamada, T., and Takai, Y. (2006). Involvement of the Ras-Ras-activated Rab5 guanine nucleotide exchange factor RIN2-Rab5 pathway in the hepatocyte growth factor-induced endocytosis of E-cadherin. J. Biol. Chem. *281*, 10598–10609.
19. Saito, K., Murai, J., Kajiho, H., Kontani, K., Kurosu, H., and Katada, T. (2002). A novel binding protein composed of homophilic tetramer exhibits unique properties for the small GTPase Rab5. J. Biol. Chem. *277*, 3412–3418.
20. Fukuda, M. (2008). Regulation of secretory vesicle traffic by Rab small GTPases. Cell. Mol. Life Sci. *65*, 2801–2813.
21. Fukuda, M. (2006). Rab27 and its effectors in secretory granule exocytosis: a novel docking machinery composed of a Rab27.effector complex. Biochem. Soc. Trans. *34*, 691–695.
22. Grosshans, B.L., Ortiz, D., and Novick, P. (2006). Rabs and their effectors: achieving specificity in membrane traffic. Proc. Natl. Acad. Sci. USA *103*, 11821–11827.
23. Carney, D.S., Davies, B.A., and Horazdovsky, B.F. (2006). Vps9 domain-containing proteins: activators of Rab5 GTPases from yeast to neurons. Trends Cell Biol. *16*, 27–35.
24. Simpson, J.C., and Jones, A.T. (2005). Early endocytic Rabs: functional prediction to functional characterization. Biochem. Soc. Symp. *72*, 99–108.
25. Barbieri, M.A., Roberts, R.L., Mukhopadhyay, A., and Stahl, P.D. (1996). Rab5 regulates the dynamics of early endosome fusion. Biocell *20*, 331–338.
26. Li, G. (1996). Rab5 GTPase and endocytosis. Biocell *20*, 325–330.
27. Loubery, S., Wilhelm, C., Hurbain, I., Neveu, S., Louvard, D., and Coudrier, E. (2008). Different microtubule motors move early and late endocytic compartments. Traffic *9*, 492–509.
28. Nielsen, E., Severin, F., Backer, J.M., Hyman, A.A., and Zerial, M. (1999). Rab5 regulates motility of early endosomes on microtubules. Nat. Cell Biol. *1*, 376–382.
29. Zerial, M., and McBride, H. (2001). Rab proteins as membrane organizers. Nat. Rev. Mol. Cell Biol. *2*, 107–117.
30. Bucci, C., Lutcke, A., Steele-Mortimer, O., Olkkonen, V.M., Dupree, P., Chiariello, M., Bruni, C.B., Simons, K., and Zerial, M. (1995). Co-operative regulation of endocytosis by three Rab5 isoforms. FEBS Lett. *366*, 65–71.
31. Gros-Louis, F., Gaspar, C., and Rouleau, G.A. (2006). Genetics of familial and sporadic amyotrophic lateral sclerosis. Biochim. Biophys. Acta *1762*, 956–972.
32. Eymard-Pierre, E., Lesca, G., Dollet, S., Santorelli, F.M., di Capua, M., Bertini, E., and Boespflug-Tanguy, O. (2002). Infantile-onset ascending hereditary spastic paralysis is associated with mutations in the alsin gene. Am. J. Hum. Genet. *71*, 518–527.
33. Hadano, S., Hand, C.K., Osuga, H., Yanagisawa, Y., Otomo, A., Devon, R.S., Miyamoto, N., Showguchi-Miyata, J., Okada, Y., Singaraja, R., et al. (2001). A gene encoding a putative GTPase regulator is mutated in familial amyotrophic lateral sclerosis 2. Nat. Genet. *29*, 166–173.
34. Yang, Y., Hentati, A., Deng, H.X., Dabbagh, O., Sasaki, T., Hirano, M., Hung, W.Y., Ouahchi, K., Yan, J., Azim, A.C., et al. (2001). The gene encoding alsin, a protein with three guanine-nucleotide exchange factor domains, is mutated in a form of recessive amyotrophic lateral sclerosis. Nat. Genet. *29*, 160–165.
35. Otomo, A., Hadano, S., Okada, T., Mizumura, H., Kunita, R., Nishijima, H., Showguchi-Miyata, J., Yanagisawa, Y., Kohiki, E., Suga, E., et al. (2003). ALS2, a novel guanine nucleotide exchange factor for the small GTPase Rab5, is implicated in endosomal dynamics. Hum. Mol. Genet. *12*, 1671–1687.

36. Topp, J.D., Carney, D.S., and Horazdovsky, B.F. (2005). Biochemical characterization of Alsin, a Rab5 and Rac1 guanine nucleotide exchange factor. Methods Enzymol. *403*, 261–276.
37. Topp, J.D., Gray, N.W., Gerard, R.D., and Horazdovsky, B.F. (2004). Alsin is a Rab5 and Rac1 guanine nucleotide exchange factor. J. Biol. Chem. *279*, 24612–24623.
38. Hennies, H.C., Kornak, U., Zhang, H., Egerer, J., Zhang, X., Seifert, W., Kuhnisch, J., Budde, B., Natebus, M., Brancati, F., et al. (2008). Gerodermia osteodysplastica is caused by mutations in SCYL1BP1, a Rab-6 interacting golgin. Nat. Genet. *40*, 1410–1412.
39. Johannes, L., and Popoff, V. (2008). Tracing the retrograde route in protein trafficking. Cell *135*, 1175–1187.
40. Colige, A., Nuytinck, L., Hausser, I., van Essen, A.J., Thiry, M., Herens, C., Ades, L.C., Malfait, F., Paepe, A.D., Franck, P., et al. (2004). Novel types of mutation responsible for the dermatosparactic type of Ehlers-Danlos syndrome (Type VIIC) and common polymorphisms in the ADAMTS2 gene. J. Invest. Dermatol. *123*, 656–663.
41. De Coster, P.J., Malfait, F., Martens, L.C., and De Paepe, A. (2003). Unusual oral findings in dermatosparaxis (Ehlers-Danlos syndrome type VIIC). J. Oral Pathol. Med. *32*, 568–570.
42. Steinmann, B., Gitzelmann, R., Vogel, A., Grant, M.E., Harwood, R., and Sear, C.H. (1975). Ehlers-Danlos syndrome in two siblings with deficient lysyl hydroxylase activity in cultured skin fibroblasts but only mild hydroxylysine deficit in skin. Helv. Paediatr. Acta *30*, 255–274.
43. Choi, J., Bergdahl, A., Zheng, Q., Starcher, B., Yanagisawa, H., and Davis, E.C. (2009). Analysis of Dermal Elastic Fibers in the Absence of Fibulin-5 Reveals Potential Roles for Fibulin-5 in Elastic Fiber Assembly. Matrix Biol., in press.
44. Boente Mdel, C., Asial, R.A., and Winik, B.C. (2006). Geroderma osteodysplastica. Report of a new family. Pediatr. Dermatol. *23*, 467–472.